PHOTONIC CRYSTAL FIBER-BASED SENSOR : DESIGN AND ANALYSIS

A DISSERTATION

SUBMITTED IN PARTIAL FULFILLMENT OF THE REQUIREMENT FOR THE AWARD OF THE DEGREE

OF

MASTER OF SCIENCE
IN

PHYSICS

Submitted by:

DEEPAK GARG | 2K22/MSCPHY/09

JYOTSNA SINGH | 2K22/MSCPHY/19

Under the supervision of

Dr. AJEET KUMAR

Assistant Professor

DEPARTMENT OF APPLIED PHYSICS

DELHI TECHNOLOGICAL UNIVERSITY

(Formerly Delhi College of Engineering)
Bawana Road, Delhi 110042

JUNE, 2024

DEPARTMENT OF APPLIED PHYSICS

DELHI TECHNOLOGICAL UNIVERSITY
(Formerly Delhi College of Engineering)
Bawana Road, Delhi 110042

CANDIDATE'S DECLARATION

We, **Deepak Garg** and **Jyotsna Singh,** hereby certify that the work which is being presented in the thesis entitled **"Photonic Crystal Fiber-Based Sensor: Design and Analysis"** in partial fulfilment of the requirements for the Degree of Master of Science in Physics, submitted to the Department of Applied Physics, Delhi Technological University, is an authentic record of our own work carried out during the period from August 2023 to June 2024 under the supervision of Dr. Ajeet Kumar.

The matter presented in the thesis has not been submitted by us for the award of any other degree of this or any other institute.

DEEPAK GARG
(2K22/MSCPHY/09)

JYOTSNA SINGH
(2K22/MSCPHY/19)

This is to certify that the students has incorporated all the corrections suggested by the examiners in the thesis and the statement made by the candidates is correct to the best of our knowledge.

DEPARTMENT OF APPLIED PHYSICS

DELHI TECHNOLOGICAL UNIVERSITY

(Formerly Delhi College of Engineering)

Bawana Road, Delhi 110042

CERTIFICATE

Certified that **Deepak Garg** (2K22/MSCPHY/09) and **Jyotsna Singh** (2K22/MSCPHY/19) has carried out their research work presented in this thesis entitled **"Photonic Crystal Fiber-Based Sensor: Design and Analysis"** for the award of **Master of Science** in Physics from Department of Applied Physics, Delhi Technological University, Delhi, under my supervision. The thesis embodies results of original work, and the studies carried out by the students themselves and the contents of the thesis do not form the basis of award of any other degree to the candidate or to anybody else from this or any other University/Institution.

Dr. AJEET KUMAR
(Assistant Professor)

ACKNOWLEDGEMENT

We are deeply grateful to our esteemed Supervisor, Dr. Ajeet Kumar, for his unwavering guidance and insightful advice, which have been crucial at every stage of this research on the applications of Photonic Crystal Fibers. His mentorship has been invaluable in shaping both the direction and success of this work. Our heartfelt thanks also go to Prof. A.S. Rao, Head of the Department of Applied Physics, for providing the essential facilities and fostering a conducive environment for our research.

We are profoundly thankful to the committee members for their critical input and suggestions, which have significantly elevated the quality of our research. We sincerely appreciate Delhi Technological University for granting us the opportunity to conduct this research and for the extensive resources and support provided.

A special note of gratitude goes to Mr. Akash Khamaru, a PhD scholar in our lab, for his constant motivation and invaluable assistance. His encouragement and help have been a continuous source of inspiration throughout our research journey.

Finally, we extend our deepest thanks to our friends and family. Their unwavering love and support have been our constant source of strength and motivation throughout this journey.

ABSTRACT

This thesis presents the design and theoretical analysis of a Photonic Crystal Fiber (PCF) based chemical sensor model. To evaluate the efficiency of this model, various optical parameters are analysed using Finite Element Method (FEM) based COMSOL Multiphysics Software. Different analytes namely Methanol (1.317), Water (1.330), Ethanol (1.354) and Benzene (1.366) have been considered for the sensing purpose in this study. The core region is infiltrated with different analytes separately. The model is simulated in THz regime (0.5 THz-1.5 THz) to evaluate optical properties. The proposed structure design exhibits a high relative sensitivity of 96.85%, 97.32%, 97.99% and 98.33% for methanol, water, ethanol, and benzene, respectively at an operating frequency of 1.3 THz. The proposed model demonstrates exceptionally low confinement loss values which are 2.22×10^{-12} dB/m for methanol, 1.16×10^{-11} dB/m for water, 1.34×10^{-11} dB/m for ethanol and is 1.30×10^{-12} dB/m for benzene. Additionally, the effective material loss for the designed PCF also comes out to be very low for all the analytes, 0.0044 cm^{-1} for methanol, 0.0040 cm^{-1} water, 0.0034 cm^{-1} for ethanol and 0.0032 cm^{-1}, for benzene. Furthermore, the PCF shows large effective mode area and numerical aperture (NA) within the mentioned range, at 1.3 THz. The NA values obtained at 1.3 THz are 0.32 for methanol, 0.40 for water, 0.32 for ethanol, and 0.32 for benzene. The obtained Effective mode Area (EMA) values are 1.46×10^{5} μm^{2} for methanol, 1.45×10^{5} μm^{2} for water, 1.44×10^{5} μm^{2} for ethanol and 1.43×10^{5} μm^{2}, for benzene. Subsequently, the optimal profile provides birefringence values of 0.0009 for methanol, 0.0010 for water, and 0.0011 for both ethanol and benzene. The practical implementation of the proposed PCF structure is possible using subsisting modern fabrication techniques.

LIST OF RESEARCH WORK AND PUBLICATIONS

Title: "Design and Performance Analysis of Octagonal Cladding Photonic Crystal Fiber for Chemical Sensing"

Author(s): Deepak Garg, Jyotsna Singh, Jaydeep Singh, Neeraj Singh, Gurmeet Singh and Ajeet Kumar

Name of Conference: Workshop on Recent Advances in Photonics (WRAP)

Date and Venue: December 7th-10th (2023), IIIT Allahabad

Status of Paper (Accepted/ Published/ Communicated): Accepted

Publish In: IEEE Explore Conference Proceedings

Date of Paper Communication: 15th September, 2023

Date of Paper Acceptance: 17th October, 2023

Title: "Design and theoretical study of Rectangular PCF based sensor for chemical sensing"

Author(s): Deepak Garg, Jyotsna Singh and Ajeet Kumar

Name of Journal: Indian Journal of Physics (Springer Nature)

Status of Paper (Accepted/ Published/ Communicated): Communicated

Date of Paper Communication: 12th April, 2024

CONTENTS

LIST OF FIGURES

LIST OF TABLES

LIST OF ABBREVIATIONS

RI	Refractive Index
FEM	Finite Element Method
PDE	Partial Differential Equation
TIR	Total Internal Reflection
PCF	Photonic Crystal Fiber
RS	Relative Sensitivity
CL	Confinement Loss
EMA	Effective mode area
EML	Effective Material Loss
PDE	Partial Differential Equation
SPR	Surface Plasmon Resonance
SPW	Surface Plasmon Wave
SPP	Surface Plasmon Polariton
PML	Perfectly matched layer
FBG	Fiber Bragg Grating

Chapter 1

INTRODUCTION

The innovation of photonic crystal fiber-based sensors has marked an advancement in the development of chemical and biomedical sensing applications owing to their exceptional optical properties [1].

Photonic crystal fibers are categorized by the presence of air holes in the cladding region along the fiber's length, creating a low effective index thus contributing to the low confinement loss. The distinctive light guiding properties of PCFs makes it compatible to design sensors [2]. The required liquid in infiltrated into the air holes, in most cases within the core; this facilitates the interaction between the targeted analyte and the light, allowing identification and examination of the unknown liquid or gas [3].

The geometric paraments of a PCF can be easy tuned by merely making changes to the shape and size of air holes, distance between the holes, material etc. [4]. For instance, a larger core facilitates better sensing application by enhancing the interaction between the light and analyte within the core [5]. Therefore, hollow core is preferred over the porous core PCF, with respect to the improved sensing capabilities.

In recent years, numerous studies have been conducted by researchers to design various PCF-based sensors tailored to specific requirements. A diverse array of sensors with unique structural designs has been proposed to meet needs. The innovations have paved a way for design of PCF-based sensors operating in different wavelength regimes. Designs with

different core-structure such as porous-core octagonal PCF [6], quasi-PCF [7-8], dual-diamond ring PCF [9] was proposed for chemical sensing in terahertz and infrared spectrum. different materials such as Topas [10], Zeonex [11], Teflon [12] and Silicon [13] have been used as background material for PCF based sensors. Material selection is an important aspect where we chose it based on its distinctive properties which fits the criteria of our study

Photonic crystal fiber sensors hold potential for applications in environmental monitoring, industrial processes, biomedicine, food preservation, and numerous other fields [14]. These sensors operate based on sophisticated and adaptable photonic crystal fiber (PCF) structures, utilizing controlled light propagation to measure amplitude, phase, polarization, and wavelength of the spectrum, along with PCF-incorporated interferometry techniques [15].

1.1 Objective of the study

The primary aim of the thesis are as follows:

- Designing a simple and practically feasible biosensor
- Study the optical properties affecting the efficiency of a sensor
- Enhance the performance and sensitivity of PCF-based sensors through innovative designs and materials
- Investigate the diverse applications of PCF-based sensors in different sectors.

1.2 Thesis Organization

- Chapter 1: This chapter provides an overview of the research work, its significance, and objectives of the study
- Chapter 2: This chapter explains the basics of PCF and its types

- Chapter 3: In this chapter we discuss different kinds of PCF-based Sensors
- Chapter 4: Overview on numerical analysis of various optical parameters
- Chapter 5: This chapter briefly talks about the optical simulation software used for the computational modelling
- Chapter 6: In this chapter, we discuss and review the obtained results, their implications and previous work
- Chapter 7: This chapter summarizes the main finding and future possibilities in the given field

Chapter 2

Photonic Crystal Fibers

Photonic crystal fibers are a type of optical fiber composed of an array of micro structured arrangement of air hole or dielectric elements along its length [16]. Introduced in the 1990s, the most prevalent form of PCF today is made from purified silica glass with air holes [17]. The region of silica embedded with the array of holes form the core of the fiber, while the region containing the air holes along the length of the fiber is called cladding [16,18]. PCFs operate as waveguide, with light guiding controlled by the periodic arrangement within the cladding.

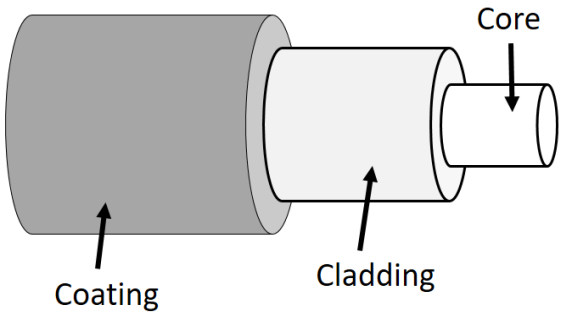

Fig1. Components of a PCF

PCFs are further categorized into two distinct types: Index-guiding and photonic band gap. The classification is based on their light-guiding mechanism. There are three types of PCFs:

i. Index-Guiding PCFs
ii. Photonic Bandgap (PBG) PCFs

2.1 Index-Guiding PCFs:

Index-guiding PCF has a solid core, surrounded by the cladding in which the air holes are arranged periodically or randomly, depending on the design [19]. They work on the same mechanism as the conventional step-index fiber. They operate on the principle of total internal reflection. Light is confined with the core, with guidance occurring because of the refractive index (RI) difference between the core and the cladding [20]. Due to the low R.I of the air holes, the core has comparatively higher R.I than cladding.

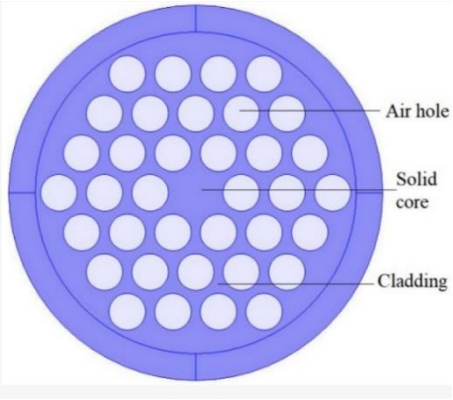

Fig.2 Design of solid-core PCF

Fig.2 illustrates the typical two-dimensional cross-section of an index-guiding photonic crystal fiber, where the center part contains the diameter of the core, diameter of the air holes is denoted by 'd', and the pitch is the distance between the air holes, usually show by Λ.

2.2 Step-Index fiber:

Step-index fibers are a type of conventional optical fiber distinguished by a constant R.I profile in both core and cladding regions. This traditional fiber setup functions according to the principle of total internal reflection, whereby light undergoes reflection at the interface of two surfaces with different refractive indices [21]. The refractive index of the core is higher than that of the cladding, leading to steep decline in refractive index at the interface

between the two regions. When the incidence angle exceeds the critical angle, a portion of the light is refracted into the medium. In step index fibers, the refractive index (n1) of the core is higher than the refractive index (n2) of the cladding [21].

Fig.3 depicts the cross-section of a traditional optical fiber in multimode and single-mode

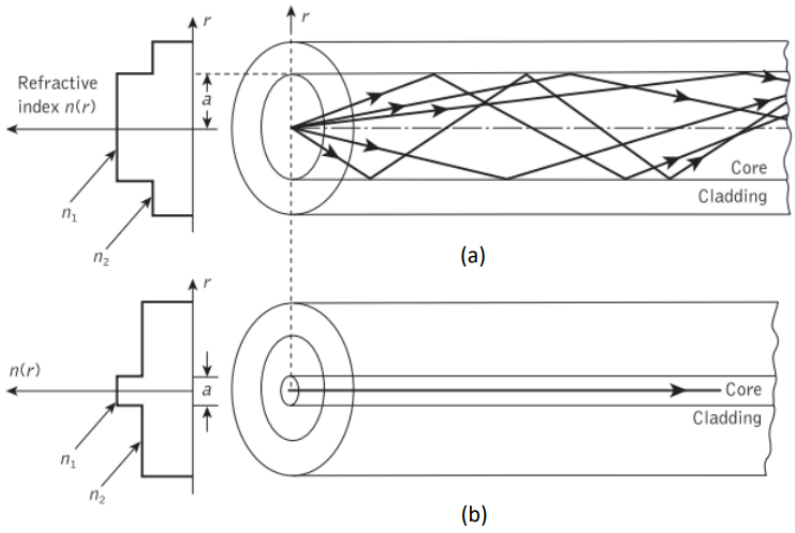

Fig.3 (a) step-index fiber in multimode; (b) step-index fiber in single-mode [22].

2.3 Photonic-Bandgap (PBG) PCFs:

Photonic bandgap fibers are a type of hollow-core PCF that works on the mechanism analogues to the principle of a periodic crystalline lattice in a semiconductor that restricts electron from occupying a bandgap region [23]. These PCFs prevent the light of a certain frequency or wavelength from propagating away from the core, holes in the cladding are arranged in a way that it reflects the light back into the core, thus confining it. These fibers provide a significant advantage by minimizing losses attributed to dielectric materials and can be employed in applications such as gas-laser transmission, pulse compression, and more [24].

Fig.4 showcases the schematic of hollow-core PCF

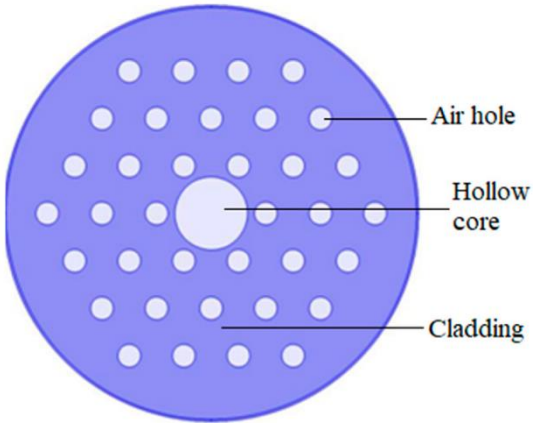

Fig.4 Hollow-Core PCF [15].

2.4 Applications

While traditional optical fibers excel in both telecommunications and non-telecommunications applications; however, they come with their own set of fundamental

limitations associated with their structures [18]. These fibers adhere to strict design criteria, including a restricted core diameter in the single-mode regime, a modal cut-off wavelength, and limited options in material as they require identical thermal properties for both the core and cladding glasses [25]. Unlike the conventional optical properties, PCFs have better guiding properties, low-loss guidance, non-linearity, higher sensitivity, high power delivery, and dispersion property [2]. The unique geometrical structure of PCFs gives us the ease and flexibility to obtain different stomata arrangement that results in different optical properties. By manipulating the parameters like the diameter of the air holes or core, pitch, refractive index, number of air holes, we can fabricate the PCFs to obtain the optimum output. Moreover, we can also design different geometrical shapes such as circle, hexagon, triangular, spiral depending upon our studies [26].

Apart from their traditional use in telecommunication, PCFs provide a wide range of application. It has been proven invaluable in the field of sensing and measurement. PCFs are widely used in making sensors of all kinds. Additionally, they are used in imaging, spectroscopy, astronomy, and more [27]. The structure is also employed in the design of optical logic gates, combinational circuits, and optical absorbers [28].

2.5 Fabrication

Various techniques and methods have been employed to fabricate different geometries of photonic crystal fibers (PCFs). For circular air holes, stacking and sol-gel methods are commonly used. The sol-gel casting method has been effectively utilized to create various micro structured fiber designs, including photonic band gap fibers, highly nonlinear fibers, and sensors and devices [29]. This casting technique offers extensive design flexibility,

essential for dispersion compensation designs and low-bend loss fibers. Additionally, the casting method is adaptable for large-scale production. Mold assemblies can be reused to cast multiple preforms, and the process can be scaled up to produce larger preform sizes, providing a cost-effective way to manufacture long lengths of uniform micro structured fiber. Drill-and-draw technology can be used to produce low-loss, porous-core honeycomb PBG THz fibers with approximately perfect hole structures [30]. For asymmetric PCF structures, extrusion and 3-D printing techniques are utilized. The extrusion method has successfully produced rectangular and spider-web-shaped PCFs, paving the way for fabricating the proposed design structure [31]

Chapter 3

Photonic Crystal Fiber- Based Sensors

The development and research on optical fiber sensors began in the 1960s [32]. Since then, optical fiber technology has been applied to a wide variety of applications. An optical fiber sensor can be defined as device which is used to measure various physical, chemical, and biological parameters by utilizing light propagating through the optical fibers [15]. The light is guided to a particular region for interaction, generating modulated optical signals containing information related to the measurable parameters.

Optical fiber sensors are highly sensitive and possess various other advantages. They are well adjusted with the communication system and compatible for performing remote sensing. Being extremely lightweight, compact size, insusceptible to the electromagnetic interference makes these sensors extremely versatile [33]. Furthermore, optical fiber sensors use dielectric instrument, making them compatible for use under harsh conditions with elevated temperature, high voltage, and corrosive environment [33].

With development of Photonic crystal fiber-based sensors there have been a breakthrough from the limitations and restrictions of the conventional fiber-based sensors. The primary constraint was the limited options of material that could be used for both the core and cladding to ensure alignment with thermal, chemical, and optical properties. The significant advantage of the PCF-based sensor was the design flexibility and porous internal structure, which for the traditional optical fibers are fixed making it difficult to manipulate the design

according to the conditions and needs [32]. Holey internal structure allows for the filling of analytes, facilitating controlled interactions between the propagating light and the analyte sample, which significantly amplifies the sensitivity of fiber optic sensors and paves the way for advanced portable sensors. PCF-based sensors demonstrate the qualities of both the optical fiber sensors and PCF itself [33].

Recent work in the PCF-based sensors development have led to an immense growth and improvement in the performance of optical fiber sensors. The progress has played a crucial role in optimizing optical amplification, laser technology, beam quality enhancement, high-power transmission, and precise core confinement with large mode areas, nonlinear functionalities, and control over group velocity dispersion.

Numerous unique biosensors have emerged for chemical sensing, fostering the development of PCF-based sensors across various wavelength ranges. Designs featuring diverse core structures, such as porous-core octagonal, hexagonal shape, square, rectangular, quasi-PCF, and dual-diamond ring PCF, have been proposed for chemical sensing in the terahertz and infrared spectra [6-9]. Additionally, chemical sensors based on surface plasmon resonance offer an effective method for detecting a wide range of unknown analytes. In this chapter we will discuss some important PCF-sensors that are popular used [34].

3.1 Plasmonic sensors

Surface plasmon resonance (SPR) occurs at the dielectric-metal interface when incident light of a specific frequency matches the oscillation frequency of conduction electrons in the metal, a condition known as phase matching. During this interaction, the guided propagation mode couples with the surface plasmon polariton (SPP) mode, resulting in a sharp loss peak

at a particular wavelength or frequency [35]. The SPR phenomenon is highly sensitive to hanges in the refractive index of the analyte; even minor deviations can cause significant shifts in the loss peak. Factors such as variations in temperature, solution concentration, applied stress or strain, and refractive index can alter the optical properties of the dielectric near the metal, leading to changes in the resonance wavelength [35].

SPR-based sensors are quite effective in the detection of unknown gas, chemicals, and liquids; thus, they have ample use in industrial and bio-medical sector. Photonic Crystal Fiber (PCF) with direct metal coating is the preferred choice for SPR sensors due to its flexibility. Recent research has utilized plasmonic materials like gold (Au), titanium dioxide (TiO2), aluminum (Al), silver (Ag), and copper (Cu) [36]. The performance of these materials in PCF is evaluated when the surface field is exposed. Silver (Ag) and gold (Au) are commonly used in SPR-based PCF sensors, with gold being more chemically stable and biocompatible, resulting in a higher peak resonance. Silver, although less stable and prone to oxidation, has a lower peak resonance, which can reduce detection accuracy [36]. Recently, a variety of innovative designs have emerged, featuring diverse methods of coating plasmonic materials. Shapes such as hexagonal, heptagonal, circular, rectangular, and D-shaped SPR-PCFs have been proposed [37-38]. Fabricating sensors with coatings inside the air holes is challenging, so structures with plasmonic material around the cladding region are generally preferred [37-38].

3.2 Terahertz Sensors

The terahertz frequency, a part of electromagnetic radiation, spans from 0.1 THz to 10 THz, situated between microwave and infrared frequencies [39]. Initially, comprehensive studies

of the THz band were impeded by transmission losses due to atmospheric moisture. To overcome this issue in THz communications, THz optical photonic crystal fibers (PCFs) have been deployed as waveguides in various applications, such as THz antennas and polarization-maintaining THz systems [40]. PCFs operating in the terahertz regime exhibit several advantageous traits; notably, THz sensors have larger core areas and fiber diameters compared to mid-infrared sensors, enhancing analyte detection. Typically, these fibers consist of hollow core, which is infused with the targeted analyte for detection. These applications include chemical sensing, alcohol detection, genetic diagnostics, time-domain spectroscopy, cancer detection, medical diagnostics, RNA analysis, and DNA analysis [40-41]. The distinctive properties of terahertz-based photonic biosensors have drawn significant attention, particularly for biomedical field. Background materials like Zeonex, Topas, and Teflon are used to achieve high relative sensitivity, low confinement loss, and excellent guiding properties. Researchers have meticulously studied THz band-based PCFs to assess guiding properties such as relative sensitivity, confinement loss, effective area, mode index, power fraction, high birefringence, and ultra-flat dispersion [42].

3.3 Interferometric PCF Sensors

PCF-sensors are a great tool to measure physical parameters such as pressure, temperature, strain and many more. Interferometric PCF sensors are one such device which is effective able to study the physical parameters [42]. These sensors combine the interferometric techniques along with the exceptional properties of PCF for various measurement. An interferometric PCF sensor leverages the unique guiding properties of photonic crystal fibers and the high sensitivity of interferometric techniques to measure a variety of physical parameters with high precision [42]. This combination makes them suitable for advanced

sensing applications in fields such as environmental monitoring, structural health monitoring, and biomedical diagnostics.

Interferometric sensors often use the core and cladding of a single-core PCF as the sensing and reference arms of an interferometer, respectively. This principle is also applied in other sensors, which can be classified based on various criteria such as the material used or the type of light-matter interaction. In dual-core or multi-core PCFs, both the interference between the fundamental modes of different cores and the interference between fundamental and higher-order modes within a core are utilized [15,43]. The length of the PCF dictates the interferometer length in sensing applications. When the effective refractive index of the modes in the sensing arm changes, these modes experience a phase shift, altering the optical path difference relative to the reference arm modes. This results in a wavelength shift in the transmission spectrum, observable as changes in the interference fringes [42-43].

3.4 Fiber Bragg Grating-Based PCF Sensor

Fiber Bragg Grating (FBG) sensors are advanced optical sensors integrated within optical fibers, designed to reflect specific wavelengths of light while transmitting others. These sensors are highly effective for monitoring physical parameters such as strain, temperature, and pressure [15]. The core of an FBG features a periodic variation in its refractive index, which acts as a wavelength-selective mirror. This periodic modulation causes light at the Bragg wavelength (λB) to be reflected through Fresnel reflection. When external conditions change, the Bragg wavelength shifts, allowing for precise measurements [42]. The period (Λ) and the number of periodic variations in the grating determine the selectivity and sensitivity of the sensor. FBG sensors are renowned for their high sensitivity, multiplexing

capabilities, and robustness in harsh environments. They find applications across diverse fields, from structural health monitoring and telecommunications to biomedical engineering, making them indispensable tools for modern sensing solutions.

Chapter 4

Numerical Analysis: Optical Parameters

In this chapter, we will discuss the important optical parameter required to be assessed for designing an effective PCF-based chemical sensor. The optical parameter assessed for the following design is effective mode index (EMI), effective material loss (EML), Effective mode area (EMA), relative sensitivity (R.S), confinement loss (C.L), and power fraction (P).

4.1 Relative Sensitivity

The relative sensitivity is the most critical component for analyzing a PCF. The relative sensitivity is the ratio that expresses about the change in the optical response of the structure compared to the change in external parameter. It is determined by the expression [41]

$$Senstivity = \frac{n_r}{n_{eff}} \times P \qquad (4.1)$$

Here, n_r represents the refractive index of the analyte, and n_{eff} represents the EMI, and P is the power fraction.

4.2 Power Fraction

Power fraction is the value which calculates the interaction between the light and the analyte present within the core. It is calculated using the equation [41]

$$P = \frac{sample \int R(E_x H_y - E_y H_x) dxdy}{whole \int R(E_x H_y - E_y H_x) dxdy} \quad (2)$$

In the above equation, E_x, E_y represents the electric field components and H_x, H_y represents the magnetic field components.

Background material is susceptible to different types of losses in the core region, primarily confinement loss and effective material loss.

4.3 Effective Mode Index

Light propagating through the fiber experiences an average refractive index determined by the design of the photonic crystal fiber, known as the effective mode index. This index can be calculated using the formula

$$n_{eff} = \frac{\beta}{k_o} \quad (4.3)$$

4.4 Confinement Loss

Confinement loss is the amount of light leaked within an optical fiber or a waveguide due to inadequate confinement of light in the core. This metric is crucial for assessing the effectiveness of optical devices, especially in photonic crystal fibers. The lower the confinement loss, the more efficient the transmission of light within the fiber. Confinement loss is evaluated by following equation [41]

$$L_c = 8.868 \times k_o l_m(n_{eff}) \frac{dB}{m} \quad (4.4)$$

k_o here is the propagation constant and $l_m(n_{eff})$ is the imaginary part of effective refractive index.

4.5 Effective Material Loss (EML)

EML is calculated by the equation [41]

$$\alpha_{eff} = \sqrt{\frac{\varepsilon_o}{\mu_o}}\left(\frac{\int n_{mat}|E|^2\alpha_{mat}dA}{|\int P_z dA|}\right) \quad (4.5)$$

Here, ε_o and μ_o is the permittivity and permeability in the free space. n_{mat} represents the refractive index and α_{mat} represents the bulk absorption loss of the TOPAS. P_z, represents the Poynting vector in z direction.

4.6 Effective Mode Area

Effective mode area (A_{eff}) is another important parameter. The effective mode area refers to the cross-sectional area through which the optical mode propagates in an optical. It is a crucial parameter that characterizes the size of the mode in the transverse direction. The effective mode area provides insights into the spatial distribution of the optical power within the waveguide. Larger value of EMA implies low value of confinement loss and high relative sensitivity. It is calculated by following formula [44]

$$A_{eff} = \frac{\left(\iint |E|^2 dxdy\right)^2}{\iint |E|^4 dxdy} \quad (4.6)$$

Chapter 5

Computational Modeling: Finite Element Method

The fields of optics, computing and simulation have been progressing at an accelerating pace. With the continuous evolution of global research, there is need for a platform or a method to study these designs extensively without bearing the brunt of expensive experimental studies. Hence, computational method and simulation method provide us with the platform to conduct the research by eliminating the need of the physical prototyping, which is both economically impractical and time-consuming. Multiphysics software such as COMSOL Multiphysics Simulation, Ansys Multiphysics, RP Fibre, and others can now create basic to intricate models of fibers and other physical designs, along with their numerical calculations. These tools enable the development of both basic and complex models, optimizing design parameters for better efficiency. Consequently, results obtained from these simulations often match experimental outcomes, demonstrating their reliability and effectiveness.

5.1 Comsol Multiphysics Software

COMSOL Multiphysics is a versatile Finite Element Method (FEM) based simulation software designed for a wide array of engineering and physics applications, particularly those involving coupled phenomena and Multiphysics. It offers an integrated development environment (IDE) and features numerous modules to address problems in electrical, mechanical, acoustics, thermodynamics, and fluid engineering. The software excels in various types of analysis, including:

a) Linear and non-linear analysis

b) Stationery and time-dependent studies

c) Frequency domain, modal, eigenfrequency, and boundary mode analysis

Additionally, COMSOL Multiphysics supports traditional physics-based user interfaces and coupled systems of partial differential equations (PDEs). It provides a unified workflow for electrical, mechanical, fluid, acoustics, and chemical applications. In the optical domain, the software comes equipped with modules for both ray and wave optics analysis. These tools enable the design and simulation of antennas, optical fibers, metamaterials, photonic waveguides, and photonic crystals. COMSOL Multiphysics is an invaluable resource for engineers and researchers, facilitating comprehensive and accurate simulations that streamline the development process and enhance innovation [45].

5.2 Finite Element Method

The Finite Element Method (FEM) is a widely used numerical technique for solving partial differential equations in 2D and 3D spaces, particularly in engineering and mathematical modeling. This method is highly effective for addressing problems in various fields, including structural analysis, heat transfer, fluid flow, mass transport, and electromagnetic potential. FEM works by breaking down complex equations into smaller, simpler parts known as finite elements. When applied to boundary value problems, FEM converts them into a system of algebraic equations that are easier to solve. These solutions are then integrated into a larger system to obtain the result. FEM's ability to simplify and solve

intricate differential equations makes it an invaluable tool in scientific and engineering applications [46].

5.1 Method of Moments

This method can be used to solve the differential equations, integral equation or the combination of both. It is also known as method of weighted residuals and is used in the computer programs that simulate the interaction between electromagnetic wave and matter. It is a frequency domain method and uses discrete meshes to convert the projection of integral equation into a system of linear equations by the application of prescribed boundary condition. The method involves four basic steps

a) The starting point is typically the derivation of the integral equation.
b) Next, the integral equation is converted into matrix equation using the weighing function and pre-defined basis function.
c) Evaluation of the matrix elements calculated in step 2.
d) Obtaining parameters of interest by solving the matrix equations.

5.2 Transfer Matrix Method (TMM)

The transfer matrix method is used in acoustics and optical domain to analyze the propagation of acoustic and electromagnetic waves through a stratified medium. According to Maxwell's equation there exist simple continuity conditions for the electric field over boundaries i.e. from one medium to another. Transfer matrix method is based on this fact only. If the field is known at some point in the space, say at the beginning then the field at the end layer of stratified medium can be predicted by performing simple matrix operations. The stack of the layers in the stratified medium can be represented as a system matrix, which is nothing but the product of all the individual layer matrices. Finally the result can be extracted by converting the system matrix into reflection and transmission coefficient.

Chapter 6

Design and theoretical study of Rectangular Photonic Crystal Fiber-based chemical sensor terahertz regime[1]

6.1 Introduction

Analysing and exploring unidentified substances is an intriguing subject in the field of science, essential for the well-being of human health. For this purpose, researchers are working diligently to develop and design different kinds of sensors which can aid in detecting unknown chemicals. Substances like alcohol and water are the most common chemicals that are used as primary components in many compound solutions. So, an effective method should be accessible for chemical sensing. Sensors based on PCFs are expected to be beneficial in industrial sectors, particularly for applications in chemical research, as well as in the fields of food and biomedical sensing [47]. In this paper, we have explored the application of chemical sensing in the terahertz regime. In the past decade, photonic crystal fibers (PCFs) operating in the terahertz region have gained tremendous popularity. Terahertz frequency belongs to the sect of electromagnetic radiation that lies in the range of microwave and infrared frequency. Terahertz radiation frequency region ranges from 0.1 THz to 10 THz [48]. A major setback that hindered the comprehensive study of the THz band earlier was the transmission loss due to the atmospheric moisture during propagation [49]. To address this problem in THz communications, THz optical photonic crystal fibers (PCFs) have been utilized as waveguides across a range of applications, encompassing THz antennas [50] and

[1] A part of this chapter has been communicated for publication in Indian Journal of Physics, Springer Nature.

polarization-maintaining THz systems [51]. PCFs operating in THz regime showcase numerous promising traits and advantages; THz sensors are bigger than the sensors operating in the mid-infrared region, in terms of core area and diameter of the fiber, thus demonstrating better analyte sensing [52].

The two key important guiding attributes for sensing and chemical sensing are confinement loss and relative sensitivity. The refractive index significantly impacts the Relative Sensitivity; a higher refractive index contrast between the core and cladding ensures the improved light confinement, resulting in increased sensitivity to changes in the surrounding environment. Birefringence of PCF is another remarkable factor taken into consideration, high value of birefringence is inherently preferred. Besides the mentioned characteristics, effective mode area (EMA), numerical aperture (NA), and effective material loss (EML) are also examined to evaluate the efficiency of the sensor.

Due to its unique geometrical structure, PCF-based devices hold an advantage over the ones based on conventional fiber. One can easily elevate the sensing of a PCF by controlling its various design parameters. The design flexibilities make PCF favourable over conventional fibers [53]. By altering the diameter and pitch of holes in the cladding and core region, we can enhance the field interaction with the analyte in the core region of the fiber. The hollow core has a prominent core volume which provides significantly better sensing than the porous-core photonic crystal fibers [54]. A greater core area enhances the interaction of light and the analyte in the core, thus helping in the sensing application.

A variety of distinct biosensors have been introduced in the last two decades for chemical sensing. The innovations have paved a way for design of PCF-based sensors operating in different wavelength regimes. Designs with different core-structure such as porous-core

octagonal PCF [55], quasi-PCF [56, 57], and dual-diamond ring PCF [58] was proposed for chemical sensing in terahertz and infrared spectrum. Chemical sensors based on Surface plasmon resonance is another effective way to obtain the sensitivity for a broad range of unknown analytes. Phase matching is a vital condition necessary for SPR, when the frequencies of light photons and electron of the plasmonic material match we observe a sharp loss peak, the fluctuation in the peak is used to identify analytes [59]. A dual-core refractive index fiber is also used for sensing application, the resonant coupling is observed between the two cores, the transmittance of the fiber changes significantly with variations in the refractive index of the surrounding medium [60].

In the past few years, different materials such as Topas [61], Zeonex [62], Teflon [63] and Silicon [64] have been used as background material for PCF based sensors. Material selection is an important aspect, and we chose it based on its distinctive properties which fits the criteria of our study. Topas and Zeonex exhibits similar properties such as constant refractive index (RI) of approximately 1.53 within THz range [65], low material loss, low dispersion, high transparency window, high transition temperatures etc. In our proposed design, we have chosen Zeonex as the bulk material. Zeonex is chosen as the background material over TOPAS and silicon due to its low absorption loss in terahertz regime (0.1-10 THz). The bulk material loss of Zeonex is 0.2 cm^{-1} [66] and the refractive index remains almost constant in the THz range. Zeonex also displays comparatively greater chemical resistivity and higher glass transition temperatures which is an essential factor for the fabrication of fiber [67].

In the past several years, many studies were conducted for the development of PCF based chemical sensors in THz frequency band. In 2023, Hossain et al. suggested a decagonal shaped PCF-based chemical sensor with hexahedron core, using Topas as the bulk material. The relative sensitivity for ethanol, benzene, and water turned out to be 92.55%, 94.65%,

90.30%, respectively. The confinement loss was measure to be 5.81×10^{-08} dB/m for ethanol, 6.01×10^{-08} dB/m for benzene, and 5.84×10^{-08} dB/m for water [52]. In the same year, Hossen et al. [68] proposed another hexahedron-shaped core, with Zeonex as the bulk material for sensing three distinct alcohols, relative sensitivity and confinement loss for ethanol was 89.50% and 5.45×10^{-08} dB/m, respectively. Ferdous et al. [69] presented an octagonal structure with a square-core. On simulation relative sensitivity for three substance water, ethanol and benzene were 90.65%, 91.93%, and 93.06%, at 1.3 THz. The confinement loss for the same substance were 2.12×10^{-13} dB/m, 2.00×10^{-13} dB/m, and 1.88×10^{-13} dB/m, respectively. In 2021, Sen et al. [70] designed a decagonal PCF with rotated-hexa core and by using Zeonex as the background material. For ethanol, water, benzene the fiber obtained values 78.56%, 79.76% and 77.51% for relative sensitivity, and for confinement loss values were 5.80×10^{-08} dB/m, 6.02×10^{-08} dB/m, and 5.74×10^{-08} dB/m, respectively. In 2020, Iqbal et al. [71] suggested a hexagonal geometry PCF using rectangular air holes for the classification and detection of alcohols. At a monitoring frequency of 2 THz, relative sensitivity for methanol was 88%, for ethanol was 91%, for propanol 92.30%, and for water it was 90.03%. Confinement loss at the optimum frequency for methanol, ethanol, propanol, and water was 0 cm^{-1}, 1.515×10^{-14} cm^{-1}, 5.935×10^{-15} cm^{-1}, and 4.045×10^{-15} cm^{-1}, respectively. In 2019, Sen et al. [72] proposed a circular design with a hexagonal core and used Silicon as the background material. The design was evaluated for ethanol, benzene, and water. At 1 THz, relative sensitivity for ethanol, benzene, and water were 76.44%, 77.16% and 73.20%, respectively. Additionally, confinement loss for the chemicals were 2.33×10^{-03} dB/m, 3.07×10^{-06} dB/m, and 2.84×10^{-02} dB/m. Recently, Kundu et al. proposed a terahertz PCF sensor for chemical identification and achieved 95.21 % for benzene and 94.67

% for ethanol and the corresponding confinement loss for benzene and ethanol are 4.674×10^{-3} dB/m and 1.378×10^{-2} dB/m [73].

The following paper presents a rectangular shaped air hole based PCF chemical sensor model. The effectiveness of the design is assessed on various optical parameters. The optical parameters are calculated for four different analytes- methanol, ethanol, benzene, and water. The model is simulated in the THz range from 0.5 THz to 1.5 THz for evaluation.

6.2 Numerical Analysis

The following study is conducted for four different analytes methanol, ethanol, benzene, and water. To assess the performance of the proposed chemical sensor, different analytes are separately injected into the rectangular core and are studied. The effectiveness of the sensor depends on various optical parameters which include, Relative sensitivity, Power fraction, Confinement loss, Effective mode area, Effective material loss, Numerical Aperture, Birefringence etc.

When light propagates through a fiber it experiences an average refractive index which is determined by the design of the PCF. This mean refractive index is referred to as the effective refractive index.

The key element for analysing the performance of a sensor is the Relative Sensitivity (RS), which is calculated by the following equation [74]:

$$RS = \frac{n_a}{n_{eff}} \times P \quad (1)$$

Where, na represents the refractive index of the analytes which is 1.317 for Methanol, 1.354 for ethanol, 1.330 for water, and 1.366 for benzene, neff stands for effective-mode index and P for power fraction.

In PCF-based chemical sensors, power fraction can be defined as the amount of propagating light that interacts with the analyte present within the core region. Power Fraction (PF) is calculated using the equation given below [75]:

$$P = \frac{sample \int R(E_x H_y - E_y H_x) dxdy}{whole \int R(E_x H_y - E_y H_x) dxdy} \quad (2)$$

In the above equation, we perform integration to calculate the light propagated within a particular analyte concerning the cross section of the fiber. Here, Ex, Ey represents the electric field components and Hx, Hy represents the magnetic field components.

Another important optical parameter which helps in the analysis of a PCF-based sensor is Confinement Loss. Confinement loss (CL) is the propagation loss due to leakage which determines the light confining ability of any PCF. The lower the confinement loss, better will be the confining ability which is a pre-requisite for any PCF based sensor model. CL depends on the imaginary part of effective mode index and is given as [75]:

$$C.L = 8.868 \times k_o I_m(n_{eff})\ dB/m \quad (3)$$

Here, k_o is the propagation constant and $I_m(n_{eff})$ is the imaginary part of the effective refractive index of fundamental mode.

Effective mode area (EMA) is also an important optical parameter in any PCF. PCFs with low effective mode area can be useful in non-linear optics and PCFs with large effective mode area can find potential applications in laser communications as well as in optical and

electronic devices. It gives the idea about the amount of light propagating in the cladding region of the fiber and in the core region where the analyte is to be filled. In a PCF-based sensor model, the high effective mode area indicates high relative sensitivity and low confinement loss. EMA which is usually referred as Aeff is calculated using the equation given below [76]:

$$A_{eff} = \frac{\left(\iint |E|^2 dxdy\right)^2}{\iint |E|^4 dxdy} \tag{4}$$

Here, |E| represents the electric field distribution of the suggested fiber sensor.

Effective material loss (EML) is another loss which comes into play during the propagation of light due to absorption by the material of the fiber. EML can be calculated as [76]:

$$\alpha_{eff} = \sqrt{\frac{\varepsilon_o}{\mu_o}}\left(\frac{\int n_{mat}|E|^2 \alpha_{mat} dA}{|\int P_z dA|}\right) \tag{5}$$

In the above equation, ε_o is the permittivity in free space and μ_o is the permeability in the free space. n_{mat} represents the refractive index and αmat represents the bulk absorption loss of the Zeonex. P_z represents the Poynting vector in the z direction.

Numerical Aperture is another important characteristic which is significant to check the efficiency of any PCF-based sensor model. Generally, a large numerical aperture is preferred for better sensing results as the higher the NA of the fiber higher the light-gathering capacity which further improves the field interaction with the analyte [77].

$$NA = \left(1 + \frac{\pi A_{eff} f^2}{c^2}\right)^{-\frac{1}{2}} \tag{6}$$

In terahertz communication systems and sensing applications, it is necessary to maintain a high polarization state. Birefringence is the property which helps in maintaining the polarization state of a fiber. Birefringence is defined as the difference in effective refractive

indices of the fundamental mode of the fiber in x and y polarizations. It can be calculated by [78]:

$$B = |n_x - n_y| \tag{7}$$

n_x and n_y here represent the effective mode indices of x-polarization and y-polarization, respectively.

6.3 Design Parameters of Proposed PCF

To study the performance of the proposed PCF sensor, the PCF model is designed using COMSOL Multiphysics software. Figure 5 represents the transverse section view of the proposed sensor model. We have considered methanol, water, ethanol, and benzene as our analytes which are to be infiltrated in the core for sensing purposes. Figure 6 represents the electric field distribution of the propagating fundamental mode in the core region at 1.3 THz. The hollow core photonic crystal fiber offers low effective material loss (EML) and provides higher sensitivity. In this model, the purple-coloured central rectangular hole acts as the core of the fiber in which different analytes are to be filled and the cladding region consists of 16 rectangular air holes which help in guiding the light to propagate through the core region. The total fiber diameter is 2.50 mm and the cladding region is adjoined with a cylindrical layer called Perfectly Matched Layer (PML) to avoid the effect of back reflections into the study area by absorbing the outgoing waves. Generally, the thickness of PML is kept between 2% to 10% of the total fiber diameter [78]. In our simulation, we considered the thickness of PML to be 9% of the fiber diameter which ensures convergence of the result. The FEM method is executed by using physics-controlled mesh. To get better simulation results we

have chosen finer mesh elements having 8742 triangular elements with 1438 edge elements and 76 vertex elements. The height and width of the core are 600 μm and 450 μm, respectively. In cladding region, six rectangles are positioned on left and right sides of the core with the same width but different heights. Identical rectangles are denoted by the same variables. In that way, the nearest rectangles to the core are denoted by R2 with height and width of 500 μm and 200 μm respectively. Similarly, the next nearest rectangles are denoted as R3 and R4 with height and width of 850 μm and 200 μm for R3 and 1025 μm and 200 μm for R4. In the vertical direction, the rectangles above the core region namely R5, R6, R7 and R8 have heights and widths of 150 μm and 1050 μm, 150 μm and 1500 μm, 200 μm and 1400 μm, 200 μm and 800 μm respectively. The pitch in the horizontal direction and vertical direction is kept constant to be 25 μm. Two similar rectangular air holes are also arranged just above and below the core to confine the propagating electric field more effectively in the core region by creating the index contrast. They are denoted as R9 and have height and width of 25 μm and 600 μm. The dimensions of the core must be kept as large as possible to get higher values of core power fraction. But keeping in mind the feasibility and fabrication complexities, we cannot choose the dimensions as per free will. In our proposed model, while simulation we have kept the width and height of the rectangular holes to be the same and varied the dimensions of the rectangular core region by 2% to experience the change in sensing performance of the model. After that, we stated the height and width of the core region as optimum (OPT). In recent times, various PCF fabrication techniques and methods have been used to fabricate different PCF geometry structures. For the fabrication of circular air holes, stacking and sol-gel methods are widely used [63-65]. Furthermore, for the fabrication of asymmetric PCF structure extrusion method and 3-D printing techniques [69-71] are used. Using the extrusion method rectangular and spider-web-shaped PCFs have

already been realized which opens up the possibility of fabrication of the proposed design structure [79]. Hence, the fabrication of the proposed PCF structure is attainable by the subsisting modern fabrication techniques.

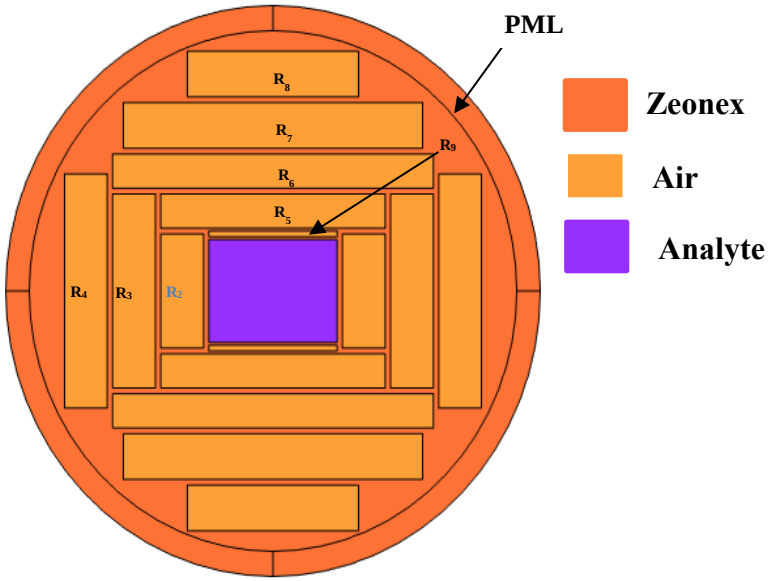

Fig.5. Proposed Structure design

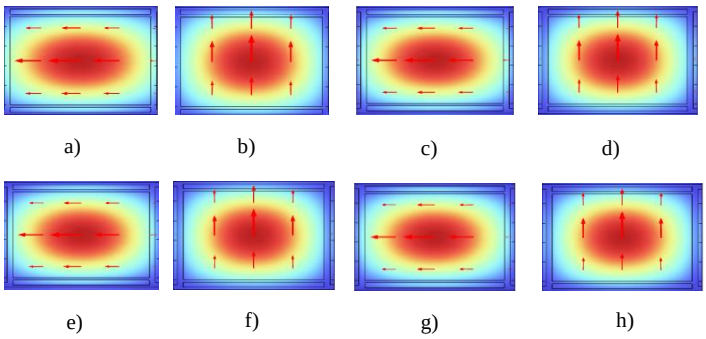

Fig.6. Mode field distribution of fundamental mode for (a) Methanol, x-pol (b) Methanol, y-pol (c) Water, x-pol (d) Water, y-pol (e) Ethanol, x-pol (f) Ethanol, y-pol (g) Benzene, x-pol (h) Benzene, y-pol

6.4 Results and Discussion

The proposed sensor model is simulated using COMSOL Multiphysics software and all the optical characteristics are calculated using the same tool. We get the results in the frequency range of 0.5-1.5 THz, and the declared optimum frequency is 1.3 THz. We have observed the Relative Sensitivity for both x and y polarization modes, PF, CL, A_{eff}, EML, NA and birefringence.

We have first analyzed the effect of frequency of the effective-mode-index of the propagating mode for all the analytes for the both polarization and shown in Figs 7-8 respectively. As expected, an increase in the effective mode index with frequency is observed for all analytes for both polarizations. As the refractive index of benzene is highest among ethanol, water and methanol hence the effective-mode-index of benzene is highest followed by ethanol, water and methanol at a particular frequency.

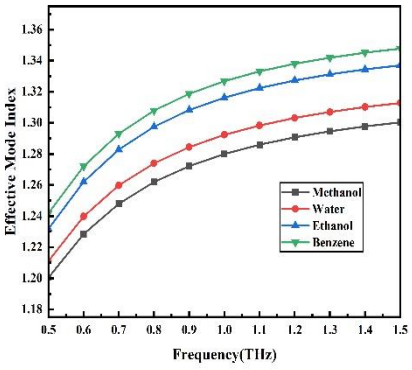

Fig.7 Effective mode index variation (x-pol)

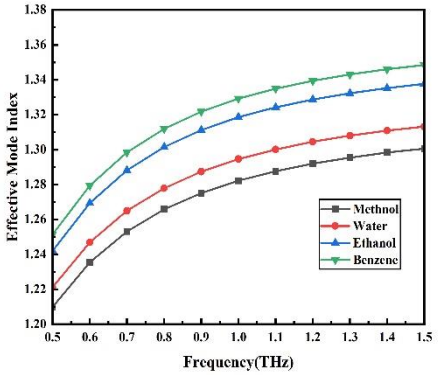

Fig.8 Effective mode index variation (y-pol)

As mentioned earlier, we have considered three different core design parameters (OPT-2%, OPT, OPT+2%). The relative sensitivities of methanol, water, ethanol and benzene as a function of frequency are shown graphically in Figs 9-14. In these figures, one can observe that RS increases with frequency. Confinement of the modal field increases with frequency and hence increases in the power fraction, *P*, thus increasing relative sensitivity. The relative sensitivity also depends proportionally on the RI of the analyte being used, as with high-index, the confinement of light is high. As a result, the relative sensitivity for benzene is highest among all analytes. Initially, the values of relative sensitivities for x polarization mode is greater than that of y polarization mode as the area of the proposed structure's core is higher in x-direction but after 1.2 THz the y polarization mode has higher relative sensitivities as light confinement becomes effective due to the presence of two nearly arranged holes in the y-direction. For OPT-2% profile, the relative sensitivities of methanol, water, ethanol and benzene are 93.46%, 94.52%, 96.03%, and 96.66% in x-polarization mode and are 94.75%, 95.46%, 96.50%, and 96.97%, respectively in y- polarization mode. For OPT profile the relative sensitivities for methanol, water, ethanol, and benzene are 96.57%, 97.15%, 97.96%, and 98.35% in x-polarization mode and are 96.85%, 97.32%, 97.99%, and 98.33% in y-polarization mode at operating frequency of 1.3 THz. For OPT+2% profile case, the calculated relative sensitivity for benzene reaches 99.34% but as we increase the length and width of the core by 2%, the chances during fabrication that the core and cladding holes get merged increase, therefore we chose the OPT profile case as a compromise. The

comparative study of the relative sensitivity of all four analytes for the y-polarization mode is shown in Table 1.

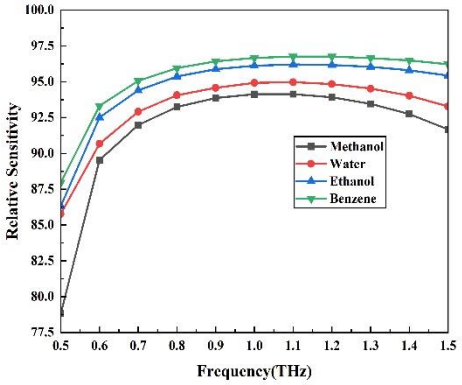

Fig.9 Relative Sensitivity for OPT-2% profile (x-pol)

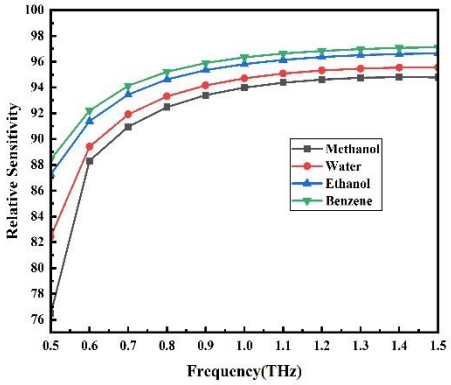

Fig.10 Relative Sensitivity for OPT-2% profile (y-pol)

Table 1

Comparative study of Relative Sensitivity of all four analytes for y polarization mode

Analyte	Profile	Operating Frequency (THz)	R.S (%)
Methanol	OPT -2%	1.3	94.75
	OPT	1.3	96.85
	OPT +2%	1.3	98.35
Water	OPT -2%	1.3	95.46
	OPT	1.3	97.32
	OPT +2%	1.3	98.66
Ethanol	OPT -2%	1.3	96.50
	OPT	1.3	97.99
	OPT +2%	1.3	99.14
Benzene	OPT -2%	1.3	96.97
	OPT	1.3	98.33
	OPT +2%	1.3	99.32

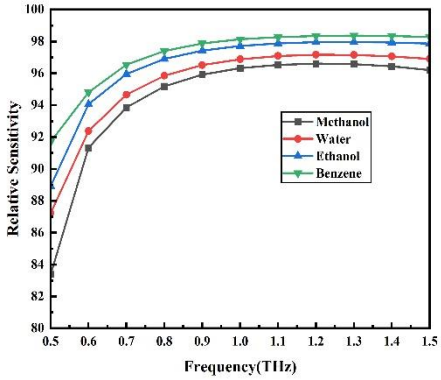

Fig.11 Relative Sensitivity for OPT profile (x-pol)

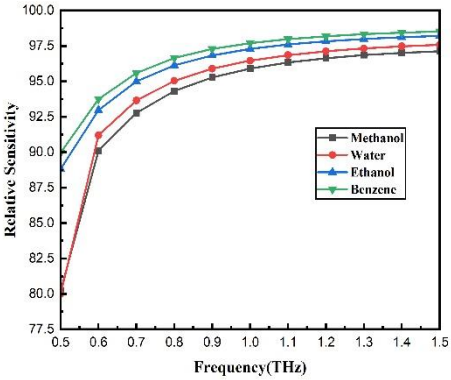

Fig.12 Relative Sensitivity for OPT profile (y-pol)

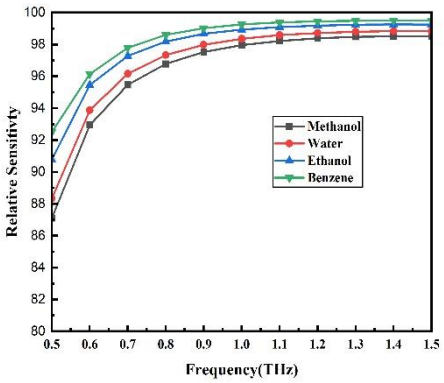

Fig.13 Relative Sensitivity for OPT+2% profile (x-pol)

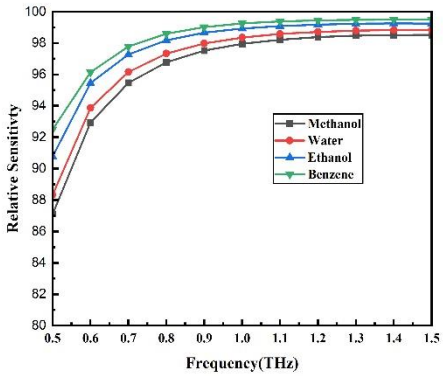

Fig.14 Relative Sensitivity for OPT+2% profile (y-pol)

Figure 15 shows the variation of Effective mode area as a function of frequency. It can be observed that the EMA of the OPT profile decreases with the increase in frequency. High operation frequency causes tight confinement of light in the core region, thus reduces the mode area of the propagating mode. At operating frequency of 1.3 THz, the values of effective mode area are 1.46×10^5 μm^2 for methanol, 1.45×10^5 μm^2 for water, 1.44×10^5 μm^2 for ethanol and 1.43×10^5 μm^2, for benzene.

Confinement loss for the OPT. profile is shown graphically as a function of frequencies in Fig.16. As the frequency increases the value of confinement loss decreases because of the

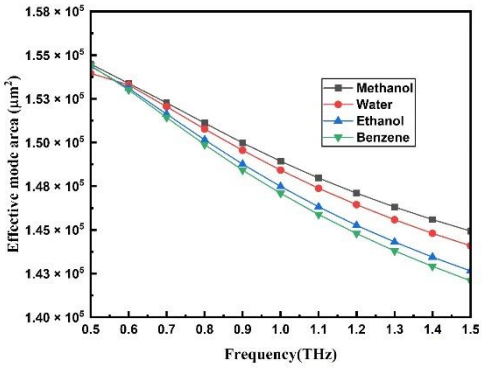

Fig.15 Effective mode area as a function of frequency

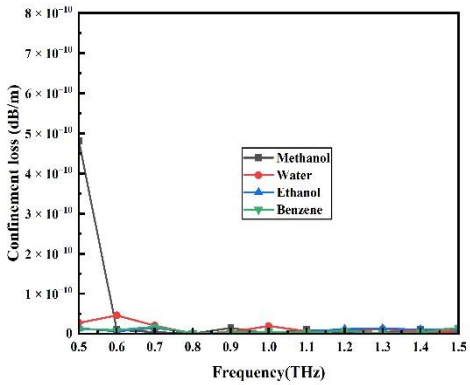

Fig.16 Confinement loss as a function of frequency

effective confinement of light at larger frequencies. Confinement loss for benzene is lowest among all other analytes as the R.I of the benzene is highest, reason being the same that light gets more confined with analytes having greater refractive indices. As observed from the graph the values below 10^{-11} dB/m are unstable reason being the values are too small and are comparable to the numerical errors introduced during the simulations [48]. The values of confinement loss at 1.3 THz are is 2.22×10^{-12} dB/m for methanol, 1.16×10^{-11} dB/m for water, 1.34×10^{-11} dB/m for ethanol and, 1.30×10^{-12} dB/m for benzene.

Effective material loss is shown graphically as a function of frequencies in Fig.17. For a PCF based sensor low EML is preferred as high values of material loss limits the sensor performance. At operating frequency region of 1.3 THz, the proposed sensor offers low values of EML which are 0.0044 cm^{-1} for methanol, 0.0040 cm^{-1} water, 0.0034 cm^{-1} for ethanol and 0.0032 cm^{-1}, for benzene.

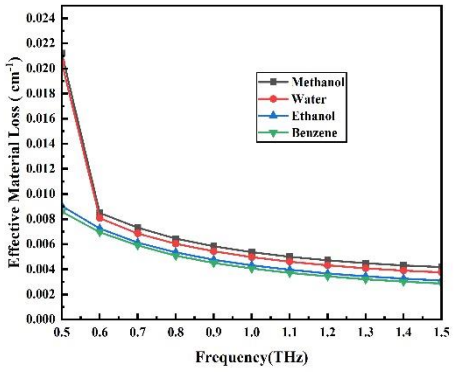

Fig.17 Effective material loss as a function of frequency

Figure 18 illustrates the birefringence as a function of frequency. Due to the asymmetry between the core and cladding air holes of the fiber, birefringence will also be present in our designed structure. Birefringence decreases as the frequency increases because the difference between the effective indices of x and y polarizations decreases with the increase in

frequency. The optimum profile offers birefringence around 0.0009 for methanol, 0.0010 for water, 0.0011 for ethanol and 0.0011, for benzene at operating frequency of 1.3 THz.

Figure 19 illustrates the variation of numerical aperture as a function of frequencies. As it is logical that NA decreases with the increase in frequency which is verified by the graph in fig.19. The obtained values of NA at 1.3 THz are 0.32 for methanol, 0.40 for water, 0.32 for ethanol and 0.32 for benzene. To get an overall idea about the performance of proposed PCF based chemical sensor model, the comparative result of the sensing properties are tabulated and represented in Table.2

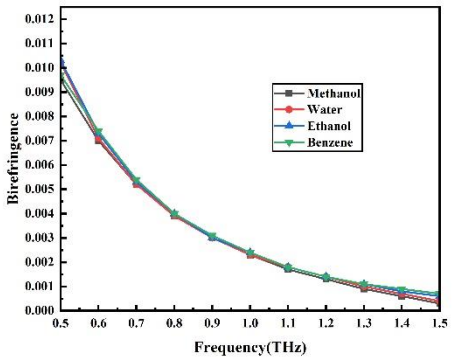

Fig.18 Birefringence as a function of frequency

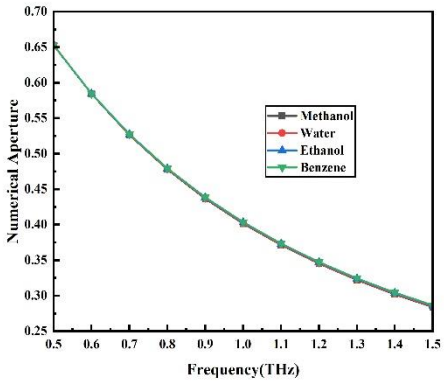

Fig.19 Numerical aperture as a function of frequency

Table 2

Comparative study of optical parameters among previous works and proposed work

Reference	Operating region (THz)	Design (Core)	Analyte	Relative Sensitivity (%)	Confinement loss (dB/m)	Material loss (cm^{-1})
[22]	1	Hexahedron	Ethanol	90.50	5.45×10^{-08}	-
[23]	1.3	Square	Water Ethanol Benzene	90.65 91.93 93.06	2.12×10^{-13} $2 .0 \times 10^{-13}$ 1.88×10^{-13}	0.0136 0.0146 0.0156
[24]	1	Rotated-hexagonal	Water Ethanol Benzene	77.51 78.56 79.76	5.74×10^{-08} 6.02×10^{-08} 5.80×10^{-08}	- - -
[25]	2	Rectangular	Methanol Water Ethanol	89.29 90.03 91.30	$0\ cm^{-1}$ 5×10^{-15} 5.9×10^{-15}	0.0056 0.0059 0.0064
[26]	1	Rotated-hexagonal	Water Ethanol Benzene	73.20 76.44 77.16	2.84×10^{-02} 2.33×10^{-03} 3.07×10^{-05}	-
[27]	-	Hexagonal	Ethanol Benzene	94.67 95.21	1.378×10^{-2} 4.674×10^{-3}	0.0083 0.0078
This paper	**1.3**	**Rectangular**	**Methanol Water Ethanol Benzene**	**96.85 97.32 97.99 98.33**	**2.22×10^{-12} 1.16×10^{-11} 1.34×10^{-11} 1.30×10^{-12}**	**0.0044 0.0040 0.0034 0.0032**

6.5 Conclusion

In conclusion, a PCF based chemical sensor with rectangular-core model is presented for its sensing application in THz region. Using Zeonex as the background material, various optical parameters of the proposed sensor model have been examined over the range of 0.5-1.5 THz. All the numerical calculations are performed by PML boundary condition using FEM based COMSOL Multiphysics software. The optimum profile of the proposed sensor model exhibits high relative sensitivities of 96.85%, 97.32%, 97.99%, 98.33%, and low values of confinement loss as 2.22×10^{-12} dB/m, 1.16×10^{-11} dB/m, 1.34×10^{-11} dB/m, 1.30×10^{-12} dB/m for methanol (1.317), water (1.33), ethanol (1.354) and benzene (1.366) respectively at 1.3 THz operating frequency. Further, effective material loss for the model also comes out to be very low which makes our proposed sensor model worthy of proficient sensing. So, the proposed PCF sensor model should be helpful in industrial areas for chemical sensing, food and biosesning applications. Furthermore, with the advancement in modern fabrication techniques, the fabrication of the proposed PCF is attainable.

Chapter 7

Conclusion and Future Work

A novel square-core photonic crystal fiber-based biosensor design has been proposed for detecting illicit drugs in blood samples, demonstrating high sensitivity and low confinement loss in the terahertz range. This sensor model, evaluated using FEM in COMSOL Multiphysics software, shows promising potential for both industrial and biomedical sensing applications. Moving forward, future efforts will focus on developing more sensitive and fabrication-friendly designs, enhancing the practicality of Surface Plasmon Resonance-based terahertz sensors for refractive index detection. Additionally, incorporating machine learning algorithms into optical fiber technology holds promise for further increasing sensor sensitivity, paving the way for real-world applications of fiber sensors. There is also potential for the development of miniaturized and portable sensor platforms, enabling real-time, on-site detection of substances of interest. This would further open opportunities for applications in fields such as environmental monitoring, food safety, and homeland security. In conclusion, we can state that the continued exploration of innovative technologies and methodologies in the field of PCF-based sensors holds immense promise to enhance the capabilities of fiber sensors and make then practically feasible for real-world applications. Additionally, leveraging advancements in nanofabrication techniques can enable the production of highly precise and consistent PCF-based sensors at a larger scale. The integration of wireless communication technologies can facilitate the development of smart sensing networks, allowing for seamless data collection and analysis. Ultimately, the

synergistic combination of novel PCF designs, state-of-the-art materials, and cutting-edge computational methods promises to revolutionize biosesning technologies, making them more accessible and impactful across various sectors.

References

1. Rachana, Maddala, Ipshitha Charles, Sandip Swarnakar, Sabbi Vamshi Krishna, and Santosh Kumar. "Recent advances in photonic crystal fiber-based sensors for biomedical applications." Optical Fiber Technology 74 (2022): 103085.
2. Islam, Mohammad Rakibul, Farhana Akter Mou, Md Moshiur Rahman, and Mohammed Imamul Hassan Bhuiyan. "Hollow core photonic crystal fiber for chemicals sensing in liquid analytes: Design and analysis." International Journal of Modern Physics B 34, no. 28 (2020): 2050259.
3. Asaduzzaman, Sayed, Kawsar Ahmed, Touhid Bhuiyan, and Tanjila Farah. "Hybrid photonic crystal fiber in chemical sensing." SpringerPlus 5 (2016): 1-11.
4. Xu, Zhongnan, Kailiang Duan, Zejin Liu, Yishan Wang, and Wei Zhao. "Numerical analyses of splice losses of photonic crystal fibers." Optics Communications 282, no. 23 (2009): 4527-4531.
5. Bahrampour, Abolfazl. "New hollow core fiber design and porphyrin thin film deposition method towards enhanced optical fiber sensors." Ph. D. dissertation, University of Naples, Italy (2013).
6. Paul, Bikash Kumar, Md Shadidul Islam, Kawsar Ahmed, and Sayed Asaduzzaman. "Alcohol sensing over O+ E+ S+ C+ L+ U transmission band based on porous cored octagonal photonic crystal fiber." Photonic Sensors 7, no. 2 (2017): 123-130.
7. Paul, Bikash Kumar, Kawsar Ahmed, Dhasarathan Vigneswaran, Fahad Ahmed, Subrata Roy, and Derek Abbott. "Quasi-photonic crystal fiber-based spectroscopic chemical sensor in the terahertz spectrum: Design and analysis." IEEE Sensors Journal 18, no. 24 (2018): 9948-9954.
8. Paul, Bikash Kumar, Kawsar Ahmed, Dhasarathan Vigneswaran, Shuvo Sen, and Md Shadidul Islam. "Quasi photonic crystal fiber for chemical sensing purpose in the terahertz regime: design and analysis." Optical and Quantum Electronics 51, no. 7 (2019): 238.
9. Paul, Bikash Kumar, Kawsar Ahmed, Hala J. El-Khozondar, Romeric F. Pobre, Joelle Sophia G. Peña, Melanie C. Merciales, Nur Aina'A. Mardhiah Zainuddin, Rozalina Zakaria, and Vigneswaran Dhasarathan. "The design and analysis of a dual-diamond-ring PCF-based sensor." Journal of Computational Electronics 19 (2020): 1288-1294.
10. Chaudhary, Vijay Shanker, and Dharmendra Kumar. "TOPAS based porous core photonic crystal fiber for terahertz chemical sensor." Optik 223 (2020): 165562.
11. Sen, Shuvo, Md Abdullah-Al-Shafi, Abu Sayed Sikder, Md Selim Hossain, and Mir Mohammad Azad. "Zeonex based decagonal photonic crystal fiber (D-PCF) in the terahertz (THz) band for chemical sensing applications." Sensing and Bio-Sensing Research 31 (2021): 100393.
12. Senthil, Revathi, Utkarsh Anand, and Prabu Krishnan. "Hollow-core high-sensitive photonic crystal fiber for liquid-/gas-sensing applications." Applied Physics A 127 (2021): 1-8.

13. Hossain, Md Selim, and Shuvo Sen. "Design and performance improvement of optical chemical sensor based photonic crystal fiber (PCF) in the terahertz (THz) wave propagation." Silicon 13, no. 11 (2021): 3879-3887.
14. Rodrigues Pinto, Ana Margarida, and Manuel López-Amo Sáinz. "Photonic crystal fibers for sensing applications." Journal of Sensors, 2012, Article ID 598178, 21 pgs. (2012).
15. De, Moutusi, Tarun Kumar Gangopadhyay, and Vinod Kumar Singh. "Prospects of photonic crystal fiber as physical sensor: an overview." Sensors 19, no. 3 (2019): 464.
16. Poli, Federica, Annamaria Cucinotta, and Stefano Selleri. Photonic crystal fibers: properties and applications. Vol. 102. Springer Science & Business Media, 2007.
17. Knight, Jonathan C. "Photonic crystal fibres." nature 424, no. 6950 (2003): 847-851.
18. Bjarklev, Anders, and Chinlon Lin. "Applications of photonic crystal fibers in optical communications-what is in the future?." In 2005 IEEE LEOS Annual Meeting Conference Proceedings, pp. 812-813. IEEE, 2005.
19. Hansen, Theis P., Jes Broeng, Stig EB Libori, Erik Knudsen, Anders Bjarklev, Jacob Riis Jensen, and Harald Simonsen. "Highly birefringent index-guiding photonic crystal fibers." IEEE Photonics Technology Letters 13, no. 6 (2001): 588-590.
20. Knight, J. C., T. A. Birks, P. St J. Russell, and J. P. De Sandro. "Properties of photonic crystal fiber and the effective index model." JOSA A 15, no. 3 (1998): 748-752.
21. Senior, J. M. "Optical Fiber Communications Principles and Practice Third Edition Optical Fiber Communications Optical Fiber Communications Principles and Practice." (2009).
22. Senior, J. M. "Optical Fiber Communications Principles and Practice Third Edition Optical Fiber Communications Optical Fiber Communications Principles and Practice." (2009).
23. Benabid, F., and P. J. Roberts. "Linear and nonlinear optical properties of hollow core photonic crystal fiber." Journal of Modern Optics 58, no. 2 (2011): 87-124.
24. Gérôme, Frédéric, Raphaël Jamier, Jean-Louis Auguste, Georges Humbert, and Jean-Marc Blondy. "Simplified hollow-core photonic crystal fiber." Optics letters 35, no. 8 (2010): 1157-1159.
25. Dragic, Peter D., M. Cavillon, and J. J. A. P. R. Ballato. "Materials for optical fiber lasers: A review." Applied Physics Reviews 5, no. 4 (2018).
26. Nizar, S. Mohamed, S. Rafi Ahamed, E. Priyanka, R. Jayasri, and B. Kesavaraman. "Comparison of different photonic crystal fiber structure: a review." In Journal of Physics: Conference Series, vol. 1717, no. 1, p. 012048. IOP Publishing, 2021.
27. Roth, Martin M., Hans-Gerd Löhmannsröben, Andreas Kelz, and Michael Kumke. "innoFSPEC: fiber optical spectroscopy and sensing." In Advanced Optical and Mechanical Technologies in Telescopes and Instrumentation, vol. 7018, pp. 1643-1650. SPIE, 2008.

28. Naghizade, Saleh, and Hamed Saghaei. "A novel design of all-optical 4 to 2 encoder with multiple defects in silica-based photonic crystal fiber." Optik 222 (2020): 165419.

29. Bise, Ryan T., and Dennis J. Trevor. "Sol-gel derived microstructured fiber: fabrication and characterization." In Optical Fiber Communication Conference, vol. 3, p. 3. Anaheim, CA, USA: Optical Society of America, 2005.

30. Bao, Hualong, Kristian Nielsen, Henrik K. Rasmussen, Peter Uhd Jepsen, and Ole Bang. "Fabrication and characterization of porous-core honeycomb bandgap THz fibers." Optics express 20, no. 28 (2012): 29507-29517.

31. Ebendorff-Heidepriem, Heike, Juliane Schuppich, Alastair Dowler, Luis Lima-Marques, and Tanya M. Monro. "3D-printed extrusion dies: a versatile approach to optical material processing." Optical Materials Express 4, no. 8 (2014): 1494-1504.

32. Sharma, Anuj K., Rajan Jha, and B. D. Gupta. "Fiber-optic sensors based on surface plasmon resonance: a comprehensive review." IEEE Sensors journal 7, no. 8 (2007): 1118-1129.

33. Zhang, Tianyu, Yu Zheng, Chengming Wang, Zhengming Mu, Yujuan Liu, and Jun Lin. "A review of photonic crystal fiber sensor applications for different physical quantities." Applied Spectroscopy Reviews 53, no. 6 (2018): 486-502.

34. Sarker, Sanchita, Dhasarathan Vigneswaran, and Filip Studnička. "Design of a nanoscale gold-coated photonic crystal fiber biosensor." Frontiers in physics 11 (2023): 1164255.

35. Islam, Mohammad Rakibul, A. N. M. Iftekher, Kazi Rakibul Hasan, Md Julkar Nayen, Saimon Bin Islam, Aadreeta Hossain, Zareen Mustafa, and Tahia Tahsin. "Design and numerical analysis of a gold-coated photonic crystal fiber based refractive index sensor." Optical and Quantum Electronics 53 (2021): 1-18.

36. Melwin, G., and K. Senthilnathan. "Modelling a simple arc shaped gold coated PCF-based SPR sensor." Journal of Optics 53, no. 1 (2024): 117-126.

37. Singh, Yadvendra, and Sanjeev Kumar Raghuwanshi. "Titanium dioxide (TiO2) coated optical fiber-based SPR sensor in near-infrared region with bimetallic structure for enhanced sensitivity." Optik 226 (2021): 165842

38. Rahman, Muntaha, Sadia Siraz, and Mariea Sharaf Anzum. "Design and performance analysis of different photonic crystal fibers." PhD diss., Department of Electrical and Electronic Engineering, Islamic University of Technology (IUT) The Organization of Islamic Cooperation (OIC) Board Bazar, Gazipur-1704, Bangladesh, 2022.

39. Bulbul, Abdullah Al-Mamun, Hasibur Rahaman, Sandipa Biswas, Md Bellal Hossain, and Abdullah-Al Nahid. "Design and numerical analysis of a PCF-based bio-sensor for breast cancer cell detection in the THz regime." Sensing and Bio-Sensing Research 30 (2020): 100388.

40. Hossain, Md Selim, Rakib Hossen, Syada Tasmia Alvi, Shuvo Sen, Md Al-Amin, and Md Mahabub Hossain. "Design and numerical analysis of a novel photonic

crystal fiber based chemicals sensor in the THz regime." Physics Open 17 (2023): 100168.

41. Sultana, Jakeya, Md Saiful Islam, Kawsar Ahmed, Alex Dinovitser, Brian W-H. Ng, and Derek Abbott. "Terahertz detection of alcohol using a photonic crystal fiber sensor." Applied optics 57, no. 10 (2018): 2426-2433.

42. Portosi, Vincenza, Dario Laneve, Mario Christian Falconi, and Francesco Prudenzano. "Advances on photonic crystal fiber sensors and applications." Sensors 19, no. 8 (2019): 1892.

43. Hou, Maoxiang, Ying Wang, Shuhui Liu, Zhihua Li, and Peixiang Lu. "Multi-components interferometer based on partially filled dual-core photonic crystal fiber for temperature and strain sensing." IEEE Sensors Journal 16, no. 16 (2016): 6192-6196.

44. Rahaman, Md Ekhlasur, Rayhan Habib Jibon, Himadri Shekhar Mondal, Md Bellal Hossain, Abdullah Al-Mamun Bulbul, and Rekha Saha. "Design and optimization of a PCF-based chemical sensor in THz regime." Sensing and Bio-Sensing Research 32 (2021): 100422.

45. Guide, Installation. "Comsol Multiphysics." 5.6, COMSOL AB (1998): 204-8.

46. Reddy, Junuthula Narasimha. An introduction to the finite element method. Vol. 3. New York: McGraw-Hill, 2005.

47. Rachana, Maddala, Ipshitha Charles, Sandip Swarnakar, Sabbi Vamshi Krishna, and Santosh Kumar. "Recent advances in photonic crystal fiber-based sensors for biomedical applications." Optical Fiber Technology 74 (2022): 103085.

48. Bulbul, Abdullah Al-Mamun, Hasibur Rahaman, Sandipa Biswas, Md Bellal Hossain, and Abdullah-Al Nahid. "Design and numerical analysis of a PCF-based bio-sensor for breast cancer cell detection in the THz regime." Sensing and Bio-Sensing Research 30 (2020): 100388.

49. Yang, Tianyu, Liang Zhang, Yunjie Shi, Shidi Liu, and Yuming Dong. "A highly birefringent photonic crystal fiber for terahertz spectroscopic chemical sensing." Sensors 21, no. 5 (2021): 1799..

50. Xin, Hao, and Min Liang. "3-D-printed microwave and THz devices using polymer jetting techniques." Proceedings of the IEEE 105, no. 4 (2017): 737-755.

51. Yang, Tianyu, Can Ding, Richard W. Ziolkowski, and Y. Jay Guo. "Circular hole ENZ photonic crystal fibers exhibit high birefringence." Optics express 26, no. 13 (2018): 17264-17278.

52. Hossain, Md Selim, Rakib Hossen, Syada Tasmia Alvi, Shuvo Sen, Md Al-Amin, and Md Mahabub Hossain. "Design and numerical analysis of a novel photonic crystal fiber based chemicals sensor in the THz regime." Physics Open 17 (2023): 100168.

53. Hu, Dora Juan Juan, and Ho Pui Ho. "Recent advances in plasmonic photonic crystal fibers: design, fabrication and applications." Advances in Optics and Photonics 9, no. 2 (2017): 257-314.

54. Islam, Mohammad Rakibul, Farhana Akter Mou, Md Moshiur Rahman, and Mohammed Imamul Hassan Bhuiyan. "Hollow core photonic crystal fiber for chemicals sensing in liquid analytes: design and analysis." International Journal of Modern Physics B 34, no. 28 (2020): 2050259.

55. Paul, Bikash Kumar, Md Shadidul Islam, Kawsar Ahmed, and Sayed Asaduzzaman. "Alcohol sensing over O+ E+ S+ C+ L+ U transmission band based on porous cored octagonal photonic crystal fiber." Photonic Sensors 7, no. 2 (2017): 123-130.

56. Paul, Bikash Kumar, Kawsar Ahmed, Dhasarathan Vigneswaran, Fahad Ahmed, Subrata Roy, and Derek Abbott. "Quasi-photonic crystal fiber-based spectroscopic chemical sensor in the terahertz spectrum: Design and analysis." IEEE Sensors Journal 18, no. 24 (2018): 9948-9954.

57. Paul, Bikash Kumar, Kawsar Ahmed, Dhasarathan Vigneswaran, Shuvo Sen, and Md Shadidul Islam. "Quasi photonic crystal fiber for chemical sensing purpose in the terahertz regime: design and analysis." Optical and Quantum Electronics 51, no. 7 (2019): 238.

58. Paul, Bikash Kumar, Kawsar Ahmed, Hala J. El-Khozondar, Romeric F. Pobre, Joelle Sophia G. Peña, Melanie C. Merciales, Nur Aina'A. Mardhiah Zainuddin, Rozalina Zakaria, and Vigneswaran Dhasarathan. "The design and analysis of a dual-diamond-ring PCF-based sensor." Journal of Computational Electronics 19 (2020): 1288-1294.

59. Sarker, Sanchita, Dhasarathan Vigneswaran, and Filip Studnička. "Design of a nanoscale gold-coated photonic crystal fiber biosensor." Frontiers in physics 11 (2023): 1164255.

60. Kamakshi, Koppole, Vipul Rastogi, and Ajeet Kumar. "Design and analysis of a refractive index sensor based on dual-core large-mode-area fiber." Optical Fiber Technology 19, no. 4 (2013): 325-329.

61. Chaudhary, Vijay Shanker, and Dharmendra Kumar. "TOPAS based porous core photonic crystal fiber for terahertz chemical sensor." Optik 223 (2020): 165562.

62. Sen, Shuvo, Md Abdullah-Al-Shafi, Abu Sayed Sikder, Md Selim Hossain, and Mir Mohammad Azad. "Zeonex based decagonal photonic crystal fiber (D-PCF) in the terahertz (THz) band for chemical sensing applications." Sensing and Bio-Sensing Research 31 (2021): 100393.

63. Senthil, Revathi, Utkarsh Anand, and Prabu Krishnan. "Hollow-core high-sensitive photonic crystal fiber for liquid-/gas-sensing applications." Applied Physics A 127 (2021): 1-8.

64. Hossain, Md Selim, and Shuvo Sen. "Design and performance improvement of optical chemical sensor based photonic crystal fiber (PCF) in the terahertz (THz) wave propagation." Silicon 13, no. 11 (2021): 3879-3887.

65. Islam, Md Saiful, Jakeya Sultana, Alex Dinovitser, Mohammad Faisal, Mohammad Rakibul Islam, Brian W-H. Ng, and Derek Abbott. "Zeonex-based asymmetrical terahertz photonic crystal fiber for multichannel communication and polarization maintaining applications." Applied optics 57, no. 4 (2018): 666-672.

66. Islam, Md Saiful, Jakeya Sultana, Alex Dinovitser, Brian W-H. Ng, and Derek Abbott. "A novel Zeonex based oligoporous-core photonic crystal fiber for polarization preserving terahertz applications." Optics Communications 413 (2018): 242-248.

67. Woyessa, Getinet, Andrea Fasano, Christos Markos, Alessio Stefani, Henrik K. Rasmussen, and Ole Bang. "Zeonex microstructured polymer optical fiber: fabrication friendly fibers for high temperature and humidity insensitive Bragg grating sensing." Optical Materials Express 7, no. 1 (2017): 286-295.

68. Hossen, Rakib, Md Selim Hossain, Sabbir Ahmed, Mohammad Sayduzzaman, Marjia Sultana, Rokaia Laizu Naima, and Shuvo Sen. "Design and performance analysis of alcohols sensing using photonic crystal fiber in terahertz spectrum." Physics Open 17 (2023): 100192.

69. Ferdous, AHM Iftekharul, Bilkis Akter, A. Priya, L. Megalan Leo, R. Thandaiah Prabu, Benjir Newaz Sathi, Diponkar Kundu et al. "Octagonal PCF with Square-Core for Surface Enhanced Spectroscopic Properties: a New Frontier in Terahertz Chemical Sensing." Plasmonics 19, no. 3 (2024): 1257-1268.

70. Sen, Shuvo, Md Abdullah-Al-Shafi, Abu Sayed Sikder, Md Selim Hossain, and Mir Mohammad Azad. "Zeonex based decagonal photonic crystal fiber (D-PCF) in the terahertz (THz) band for chemical sensing applications." Sensing and Bio-Sensing Research 31 (2021): 100393.

71. Iqbal, Faysal, Sandipa Biswas, Abdullah Al-Mamun Bulbul, Hasibur Rahaman, Md Bellal Hossain, Md Ekhlasur Rahaman, and Md Abdul Awal. "Alcohol sensing and classification using PCF-based sensor." Sensing and Bio-Sensing Research 30 (2020): 100384.

72. Sen, Shuvo, and Kawsar Ahmed. "Design of terahertz spectroscopy based optical sensor for chemical detection." SN Applied Sciences 1, no. 10 (2019): 1215.

73. Rahaman, Md Ekhlasur, Himadri Shekhar Mondal, Md Bellal Hossain, Md Mahbub Hossain, Md Shamim Ahsan, and Rekha Saha. "Simulation of a highly birefringent photonic crystal fiber in terahertz frequency region." SN Applied Sciences 2 (2020): 1-7.

74. Islam, Md Saiful, Jakeya Sultana, Alex Dinovitser, Brian W-H. Ng, and Derek Abbott. "A novel Zeonex based oligoporous-core photonic crystal fiber for polarization preserving terahertz applications." Optics Communications 413 (2018): 242-248.

75. Russell, Philip St J. "Photonic-crystal fibers." Journal of lightwave technology 24, no. 12 (2006): 4729-4749.

76. El Hamzaoui, Hicham, Youcef Ouerdane, Laurent Bigot, Géraud Bouwmans, Bruno Capoen, Aziz Boukenter, Sylvain Girard, and Mohamed Bouazaoui. "Sol-gel derived ionic copper-doped microstructured optical fiber: a potential selective ultraviolet radiation dosimeter." Optics express 20, no. 28 (2012): 29751-29760.

77. Atakaramians, Shaghik, Shahraam Afshar, Heike Ebendorff-Heidepriem, Michael Nagel, Bernd M. Fischer, Derek Abbott, and Tanya M. Monro. "THz porous fibers: design, fabrication and experimental characterization." Optics express 17, no. 16 (2009): 14053-14062.

78. Ebendorff-Heidepriem, Heike, Juliane Schuppich, Alastair Dowler, Luis Lima-Marques, and Tanya M. Monro. "3D-printed extrusion dies: a versatile approach to optical material processing." Optical Materials Express 4, no. 8 (2014): 1494-1504.

79. Rani, K. Renuka, and K. Chitra. "Design and analysis of low loss solid-core hexagonal photonic crystal fiber for applications in terahertz regime." In Journal of Physics: Conference Series, vol. 2426, no. 1, p. 012019. IOP Publishing, 2023.

Appendix 2

Similarity Report

PAPER NAME

Dissertation II (Jyotsna Singh) Plagiarism Report-12-52.pdf

WORD COUNT	CHARACTER COUNT
7461 Words	**43077 Characters**
PAGE COUNT	FILE SIZE
41 Pages	**1.3MB**
SUBMISSION DATE	REPORT DATE
Jun 6, 2024 7:39 PM GMT+5:30	**Jun 6, 2024 7:40 PM GMT+5:30**

6% Overall Similarity

The combined total of all matches, including overlapping sources, for each database.

- 3% Internet database
- 4% Publications database
- Crossref database
- Crossref Posted Content database
- 2% Submitted Works database

Excluded from Similarity Report

- Bibliographic material
- Quoted material
- Cited material
- Small Matches (Less then 12 words)

Summary